2005 American Control Conference
June 8-10, 2005. Portland, OR, USA

Broadband Adaptive Disturbance Rejection for a Deployable Optical Telescope Testbed

Jesse B. Hoagg[1], Seth L. Lacy[2] and Dennis S. Bernstein[3]

Abstract— **Broadband adaptive disturbance rejection is demonstrated on the artificial white-light source of the Deployable Optical Telescope (DOT) developed by the Air Force Research Laboratory (AFRL). Large deployable optical systems are envisioned as the future of space telescopes. These systems will require active control for disturbance rejection. In this paper, we consider a multi-input, multi-output discrete-time adaptive disturbance rejection algorithm. The algorithm requires knowledge of some Markov parameters of the system from the control signal inputs to the performance variables. No information about the disturbance spectrum is required. We demonstrate broadband disturbance rejection numerically on an identified model of DOT's white-light source and experimentally on the system itself.**

1. Introduction

Deployable space telescopes offer a viable method for placing large aperture optical systems into space. To explore the issues associated with fielding a lightweight deployable telescope, the Air Force Research Laboratory (AFRL) developed the Deployable Optical Telescope (DOT) [1–3]. DOT is a fully deployable, ground-based, space-traceable optical telescope. DOT uses laser metrology to provide optical-precision measurements and active feedback control to reject disturbances to the telescope's alignment. In addition, ground-based testing requires a pseudo-star or artificial white-light source that is fixed relative to the telescope. In the laboratory, the artificial white-light source is subject to ambient disturbances, and requires a method of disturbance rejection to ensure that it is stationary relative to the telescope. Furthermore, the testing requires a disturbance rejection algorithm based on minimal modeling information and without specific knowledge of the disturbance spectrum. These requirements necessitate adaptive disturbance rejection.

Adaptive feedforward control is frequently used to reject harmonic disturbances when the disturbance frequencies are known or can be estimated [4–7]. Adaptive feedforward algorithms typically rely on least-mean-square (LMS) or recursive least-mean-square (RLMS) algorithms to update parameters. These methods include the filtered-u LMS and filtered-x LMS algorithms. However, adaptive feedforward algorithms do not account for the transfer function from the control signals to the measurements.

[1]National Defense Science and Engineering Graduate Fellow, Department of Aerospace Engineering, The University of Michigan, Ann Arbor, MI 48109-2140, phone: (734) 763-1305, fax: (734) 763-0578, email: jhoagg@umich.edu

[2]Air Force Research Laboratory, Space Vehicles Directorate, Kirtland AFB, NM 87117-5776

[3]Professor, Department of Aerospace Engineering, The University of Michigan, Ann Arbor, MI 48109-2140

As an alternative, we consider adaptive feedback disturbance rejection [8, 9]. In [8], an adaptive feedback disturbance rejection algorithm is developed based on a retrospective performance measure. The retrospective performance of a system is the performance of the system at the current time assuming that the current controller was used over a past window of time. In [8], the retrospective performance measure is used in connection with time-series modeling of the plant and the controller to develop an adaptive disturbance rejection algorithm that requires knowledge of only the numerator of the transfer function from the control to the performance measurement.

In [9], the authors adopt a retrospective performance measure and develop an adaptive disturbance rejection algorithm based on a state-space model of the plant. The algorithm requires knowledge of Markov parameters from the control to the performance, rather than the numerator of this transfer function as in [8].

In the present paper, we implement the retrospective cost adaptive disturbance rejection algorithm of [9] on the artificial white-light source system for AFRL's DOT testbed. Using this algorithm, we demonstrate broadband adaptive disturbance rejection on a multi-input, multi-output system with limited model information and no knowledge of the disturbance spectrum.

In Section 2, we formulate the disturbance rejection problem and rewrite the performance variable in terms of Markov parameters. In Section 3, we review the adaptive feedback disturbance rejection controller presented in [9]. In Section 4, we describe the DOT testbed. Numerical simulations of the DOT testbed and the adaptive controller are given in Section 5. Section 6 provides the experimental results, and conclusions are given in Section 7.

2. Disturbance Rejection Problem Formulation

Consider the linear shift-invariant discrete-time system

$$x(k+1) = Ax(k) + Bu(k) + D_1 w(k), \tag{2.1}$$

$$z(k) = E_1 x(k) + E_2 u(k) + E_0 w(k), \tag{2.2}$$

$$y(k) = Cx(k) + Du(k) + D_2 w(k), \tag{2.3}$$

where $x(k) \in \mathbb{R}^n$, $u(k) \in \mathbb{R}^{l_u}$, $w(k) \in \mathbb{R}^{l_w}$, $y(k) \in \mathbb{R}^{l_y}$, and $z(k) \in \mathbb{R}^{l_z}$. We assume that A is an asymptotically stable matrix. The standard disturbance rejection problem has two input signals and two output signals. The inputs are the disturbance $w(k)$ and the control $u(k)$. The outputs are the measurement $y(k)$ and the performance $z(k)$. The objective of feedback disturbance rejection is to determine a

control $u(k)$ using the measurement $y(k)$ that minimizes the performance $z(k)$ in the presence of the external disturbance $w(k)$. We assume that $w(k)$ is not measured.

Propagating the state backwards for q time steps, equations (2.1) and (2.2) can be combined to yield

$$\begin{aligned} z(k) &= E_1 A^q x(k-q) \\ &\quad + \begin{bmatrix} H_0 & H_1 & \cdots & H_q \end{bmatrix} \begin{bmatrix} u(k) \\ u(k-1) \\ \vdots \\ u(k-q) \end{bmatrix} \\ &\quad + \begin{bmatrix} \hat{H}_0 & \hat{H}_1 & \cdots & \hat{H}_q \end{bmatrix} \begin{bmatrix} w(k) \\ w(k-1) \\ \vdots \\ w(k-q) \end{bmatrix}. \end{aligned} \tag{2.4}$$

The Markov parameters from the disturbance $w(k)$ to the performance $z(k)$ are given by $\hat{H}_0 \triangleq E_0$ and, for $i = 1, \ldots, q$, $\hat{H}_i \triangleq E_1 A^{i-1} D_1$. Furthermore, the Markov parameters from the control $u(k)$ to the performance $z(k)$ are given by $H_0 \triangleq E_2$ and, for $i = 1, \ldots, q$, $H_i \triangleq E_1 A^{i-1} B$.

Next, we define the retrospective performance window $p > 0$. For all $j = 0, \ldots, p-1$, the performance is

$$\begin{aligned} z(k-j) &= E_1 A^q x(k-q-j) \\ &\quad + \begin{bmatrix} H_0 & H_1 & \cdots & H_q \end{bmatrix} \begin{bmatrix} u(k-j) \\ u(k-1-j) \\ \vdots \\ u(k-q-j) \end{bmatrix} \\ &\quad + \begin{bmatrix} \hat{H}_0 & \hat{H}_1 & \cdots & \hat{H}_q \end{bmatrix} \begin{bmatrix} w(k-j) \\ w(k-1-j) \\ \vdots \\ w(k-q-j) \end{bmatrix}. \end{aligned} \tag{2.5}$$

We define the performance block vector $Z(k)$, the disturbance block vector $W(k)$, and the control block vector $U(k)$ by

$$Z(k) \triangleq \begin{bmatrix} z(k) \\ \vdots \\ z(k-p+1) \end{bmatrix}, \tag{2.6}$$

$$W(k) \triangleq \begin{bmatrix} w(k) \\ \vdots \\ w(k-p-q+1) \end{bmatrix}, \tag{2.7}$$

$$U(k) \triangleq \begin{bmatrix} u(k) \\ \vdots \\ u(k-p-q+1) \end{bmatrix}. \tag{2.8}$$

Equation (2.5) implies

$$\begin{aligned} Z(k) &= \begin{bmatrix} E_1 A^q x(k-q) \\ \vdots \\ E_1 A^q x(k-q-p+1) \end{bmatrix} \\ &\quad + H_{zu} U(k) + H_{zw} W(k), \end{aligned} \tag{2.9}$$

where $H_{zw} \in \mathbb{R}^{pl_z \times (p+q) l_w}$ and $H_{zu} \in \mathbb{R}^{pl_z \times (p+q) l_u}$ are given by

$$H_{zw} \triangleq \begin{bmatrix} \hat{H}_0 & \cdots & \hat{H}_q & 0_{l_z \times l_w} & \cdots & 0_{l_z \times l_w} \\ 0_{l_z \times l_w} & \ddots & & \ddots & \ddots & \vdots \\ \vdots & & \ddots & & \ddots & 0_{l_z \times l_w} \\ 0_{l_z \times l_w} & \cdots & 0_{l_z \times l_w} & \hat{H}_0 & \cdots & \hat{H}_q \end{bmatrix}, \tag{2.10}$$

$$H_{zu} \triangleq \begin{bmatrix} H_0 & \cdots & H_q & 0_{l_z \times l_u} & \cdots & 0_{l_z \times l_u} \\ 0_{l_z \times l_u} & \ddots & & \ddots & \ddots & \vdots \\ \vdots & & \ddots & & \ddots & 0_{l_z \times l_u} \\ 0_{l_z \times l_u} & \cdots & 0_{l_z \times l_u} & H_0 & \cdots & H_q \end{bmatrix}. \tag{2.11}$$

3. Adaptive Feedback Disturbance Rejection

For adaptive feedback disturbance rejection, consider the controller

$$u(k) = \sum_{i=1}^{n_c} -a_{c_i}(k) u(k-i) + \sum_{i=1}^{n_c} b_{c_i}(k) y(k-i), \tag{3.1}$$

where, for $i = 1, \ldots, n_c$, $a_{c_i}(k) \in \mathbb{R}^{l_u \times l_u}$ and $b_{c_i}(k) \in \mathbb{R}^{l_u \times l_y}$. We define the controller parameter matrix

$$\theta(k) \triangleq \begin{bmatrix} -a_{c_1}(k) & \cdots & -a_{c_{n_c}}(k) & b_{c_1}(k) & \cdots & b_{c_{n_c}}(k) \end{bmatrix}, \tag{3.2}$$

and the regressor

$$\Phi_{uy}(k) \triangleq \begin{bmatrix} u(k-1) \\ \vdots \\ u(k-n_c-q-p+1) \\ y(k-1) \\ \vdots \\ y(k-n_c-q-p+1) \end{bmatrix}, \tag{3.3}$$

where $\theta(k) \in \mathbb{R}^{l_u \times n_c (l_u + l_y)}$ and $\Phi_{uy}(k) \in \mathbb{R}^{(l_u+l_y)(n_c+q+p-1)}$. The controller (3.1) can be written in terms of (3.2) and (3.3) as

$$u(k) = \theta(k) R_1 \Phi_{uy}(k), \tag{3.4}$$

where, for $i = 1, \ldots, q+p$, $R_i \in \mathbb{R}^{n_c(l_u+l_y) \times (l_u+l_y)(n_c+p+q-1)}$ is given by

$$R_i \triangleq \begin{bmatrix} 0_{n_c l_u \times (i-1) l_u} & I_{n_c l_u} & 0_{n_c l_u \times ((p-i) l_u + (i-1) l_y)} \\ 0_{n_c l_y \times (i-1) l_u} & 0_{n_c l_y \times n_c l_u} & 0_{n_c l_y \times ((p-i) l_u + (i-1) l_y)} \\ 0_{n_c l_u \times n_c l_y} & 0_{n_c l_u \times (p-i) l_y} \\ I_{n_c l_y} & 0_{n_c l_y \times (p-i) l_y} \end{bmatrix} \tag{3.5}$$

Similarly, the control block vector can be expressed as

$$U(k) = \sum_{i=1}^{p+q} L_i \theta(k-i+1) R_i \Phi_{uy}(k), \tag{3.6}$$

where

$$L_i \triangleq \left[\begin{array}{c} 0_{(i-1)l_u \times l_u} \\ I_{l_u} \\ 0_{(p+q-i)l_u \times l_u} \end{array} \right] \in \mathbb{R}^{(p+q)l_u \times l_u}. \tag{3.7}$$

Therefore, the performance block vector (2.9) can be written as

$$Z(k) = H_{zu} \sum_{i=1}^{p+q} L_i \theta(k-i+1) R_i \Phi_{uy}(k) + H_{zw} W(k) + \left[\begin{array}{c} E_1 A^q x(k-q) \\ \vdots \\ E_1 A^q x(k-q-p+1) \end{array} \right]. \tag{3.8}$$

The retrospective performance block vector is defined as

$$\hat{Z}(k) \triangleq H_{zu} \sum_{i=1}^{p+q} L_i \theta(k) R_i \Phi_{uy}(k) + H_{zw} W(k) + \left[\begin{array}{c} E_1 A^q x(k-q) \\ \vdots \\ E_1 A^q x(k-q-p+1) \end{array} \right]. \tag{3.9}$$

By combining (2.9) and (3.9), we obtain

$$\hat{Z}(k) = Z(k) - H_{zu} U(k) + H_{zu} \sum_{i=1}^{p+q} L_i \theta(k) R_i \Phi_{uy}(k). \tag{3.10}$$

Define the retrospective performance cost function

$$J(k) \triangleq \frac{1}{2} \hat{Z}^{\mathrm{T}}(k) \hat{Z}(k). \tag{3.11}$$

The gradient with respect to the controller parameters is given by

$$\frac{\partial J(k)}{\partial \theta(k)} = \sum_{i=1}^{q+p} L_i^{\mathrm{T}} H_{zu}^{\mathrm{T}} \hat{Z}(k) \Phi_{uy}^{\mathrm{T}}(k) R_i^{\mathrm{T}}. \tag{3.12}$$

Therefore, the controller gradient update law is

$$\theta(k+1) = \theta(k) - \eta(k) \frac{\partial J(k)}{\partial \theta(k)}, \tag{3.13}$$

where

$$\eta(k) \triangleq \frac{1}{(p+q)\, ||H_{zu}||_F^2\, ||\Phi_{uy}(k)||_2^2}. \tag{3.14}$$

In [8, 9], it is shown that the adaptive law (3.13)-(3.14) guarantees that the controller parameters asymptotically approach optimal values.

Fig. 1. The Deployable Optical Telescope (DOT) testbed.

4. Experimental Setup

The Deployable Optical Telescope (DOT) was developed by the Air Force Research Laboratory to explore the issues associated with lightweight deployable space structures. DOT is a fully deployable, ground-based, sub-scale, space-traceable testbed [1–3]. Specifically, DOT is a sparse-array telescope with three deployable primary mirror segments, a deployable secondary tower, and a laser metrology system. DOT is shown in Figure 1

For ground-based testing, an artificial white-light source, often called a pseudo-star, is required to calibrate an optical telescope's feedback control system. The DOT testbed includes an artificial white-light source mounted at the top of the metrology tower shown in Figure 2. For space-based calibration, a white-light source, which is fixed relative to the optical telescope, is chosen. However, for ground-based testing, the artificial white-light source is susceptible to exogenous disturbances such as ambient vibrations and thermal variations. In particular, the dynamics of DOT's metrology tower cause motion of the artificial white-light source. Motion of the artificial white-light source couples into the optical path so that motion of the telescope cannot be distinguished from the motion of the artificial white-light source. Hence, the artificial white-light source must be actively controlled to reject disturbances of the source relative to the optical telescope.

A diode laser and optical sensor serve are the feedback for the artificial white-light source system. The diode laser

Fig. 2. The metrology tower for the DOT testbed.

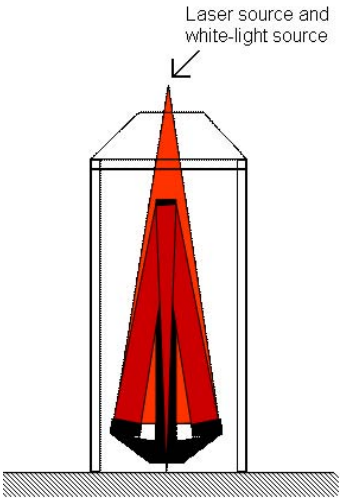

Fig. 3. The diode laser beam and artificial white-light enter the telescopes optical path at a point above the secondary tower.

is mounted at the top of the metrology tower in line with the white light point source. In addition, a fast-steering mirror is also mounted at the top of the metrology tower. The white-light source and the laser reflect off of the fast-steering mirror and enters the optical path of the telescope. Figure 3 shows how the laser beam and white-light enter the telescopes optical path. An optical sensor, model OT-301, manufactured by On-Trak Photonics, Inc., Lake Forest, CA, is located at the base of the optical telescope. This sensor provides displacement measurements of the laser beam and the white-light source along two orthogonal directions relative to the floor of the laboratory. Hence, the optical sensor measures displacement of the light source entering the telescope's optical path relative to the base of the telescope. These two measurements comprise the performance variables $z(k)$. In addition, 2-axis displacement measurements of the fast-steering mirror are available. All four available measurements are used for the feedback measurement $y(k)$. The tip and tilt of the fast-steering mirror are the control inputs $u(k)$.

5. Numerical Results

In this section, we simulate the artificial white-light source system controlled by the adaptive disturbance rejection algorithm presented in Section 3. The numerical results are obtained from Matlab using an identified model of the artificial white-light source system. The system's control inputs are the tip and tilt of the fast-steering mirror, and the four outputs are the 2-axis displacements of the fast-steering mirror and 2-axis measurement from the optical sensor. The system is excited with sinesweep inputs to each control channel, and a 12th-order state-space model is identified from the input and output data. The identified model is obtained from a frequency domain subspace identification method [10]. The discrete-time identified model can be represented by (2.1)-(2.3) where

$$A = \text{diag}\left(\begin{bmatrix} 0.90 & 0.29 \\ -0.29 & 0.90 \end{bmatrix}, \begin{bmatrix} 0.90 & 0.28 \\ -0.28 & 0.90 \end{bmatrix}, \begin{bmatrix} 0.86 & 0.50 \\ -0.50 & 0.86 \end{bmatrix}, \begin{bmatrix} 0.90 & 0.43 \\ -0.43 & 0.90 \end{bmatrix}, \begin{bmatrix} 0.93 & 0.35 \\ -0.35 & 0.93 \end{bmatrix}, \begin{bmatrix} 0.92 & 0.39 \\ -0.39 & 0.92 \end{bmatrix}\right), \tag{5.1}$$

$$B = \begin{bmatrix} -0.97 & -0.24 \\ -0.82 & -0.29 \\ 0.34 & -0.76 \\ -0.27 & 0.89 \\ 0.011 & 0.018 \\ -0.0240 & -0.027 \\ 0.0029 & 0.014 \\ -0.027 & -0.039 \\ 0.026 & 0.057 \\ -0.099 & -0.074 \\ -0.0034 & 0.016 \\ -0.037 & -0.055 \end{bmatrix}, \tag{5.2}$$

$$E_2 = \begin{bmatrix} 2.3 \times 10^{-5} & -2.6 \times 10^{-4} \\ -1.9 \times 10^{-4} & -1.1 \times 10^{-5} \end{bmatrix}, \tag{5.3}$$

$$D = \begin{bmatrix} 8.5 \times 10^{-5} & 2.8 \times 10^{-5} \\ 7.3 \times 10^{-5} & 1.9 \times 10^{-4} \\ 2.3 \times 10^{-5} & -2.6 \times 10^{-4} \\ -1.9 \times 10^{-4} & -1.1 \times 10^{-5} \end{bmatrix}. \tag{5.4}$$

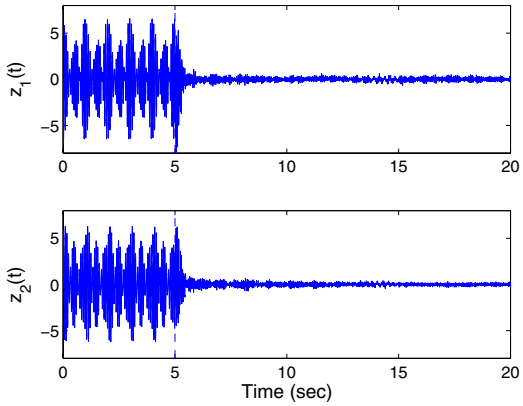

Fig. 4. Time trace of the simulation performance variables. At 5 seconds, the adaptive controller is turned on and rejects the disturbance containing multiple tones and broadband white noise.

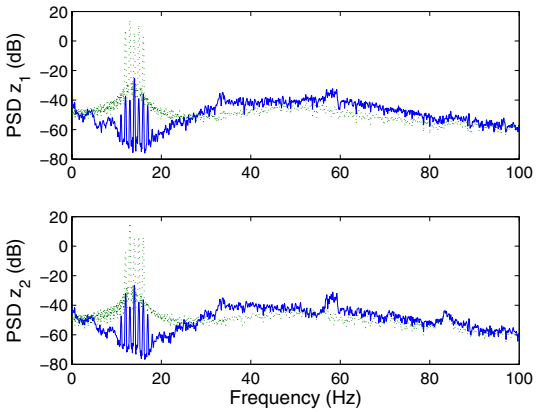

Fig. 5. Open-loop (dotted) and closed-loop (solid) power spectral densities of the simulation performance variables.

$$E_1 = \left[\begin{array}{ccccccc} 0.081 & -0.067 & 0.094 & 0.091 & 0.00097 & 0.0018 & -0.00014 \\ -0.10 & 0.10 & 0.029 & 0.042 & -0.011 & -0.0092 & -0.0050 \\ 2.6\times10^{-5} & 0.00089 & 0.0033 & -1.9\times10^{-5} & -0.00062 & & \\ -0.0031 & -0.012 & -0.012 & -0.011 & -0.0095 & & \end{array} \right], \tag{5.5}$$

$$C = \left[\begin{array}{ccccccc} 0.17 & -0.16 & 0.066 & 0.052 & 0.012 & 0.011 & 0.0045 \\ 0.046 & -0.065 & -0.17 & -0.19 & 0.016 & 0.015 & 0.0067 \\ 0.081 & -0.067 & 0.094 & 0.091 & 0.00097 & 0.0018 & -0.00014 \\ -0.10 & 0.10 & 0.029 & 0.042 & -0.011 & -0.0092 & \\ 0.0033 & 0.012 & 0.014 & 0.0099 & 0.0085 & & \\ 0.0060 & 0.016 & 0.013 & 0.016 & 0.016 & & \\ 2.6\times10^{-5} & 0.00089 & 0.0033 & -1.9\times10^{-5} & -0.00062 & & \\ -0.0031 & -0.012 & -0.012 & -0.011 & -0.0095 & & \end{array} \right], \tag{5.6}$$

Furthermore, we construct a realistic disturbance spectrum that replicates the true disturbances seen by the artificial white-light source system. The disturbance input matrices are $E_0 = 0$, $D_2 = 0$, and $D_1 \in \mathbb{R}^{12\times5}$ is a matrix of independent random variables uniformly distributed on the interval $[-1, 1]$. The disturbance signal is chosen to be a combination of densely spaced tones and band-limited white-noise. The five disturbance inputs are sinusoids at frequencies 12, 13, 14, 15, and 16 Hz, respectively, combined with white-noise band-limited up to 100 Hz.

The system (2.1)-(2.3) and (5.1)-(5.6) is simulated with the adaptive disturbance rejection implemented in the feedback loop with $n_c = 200$, $p = 5$, and $q = 4$. The initial conditions of the artificial white-light system are assumed to be zero. Similarly, the adaptive controller is initialized with zero initial condition. Figure 4 shows the disturbance rejection in the time-domain. For 5 seconds, the system operates in open loop. Then the disturbance rejection algorithm is turned on and rejects the disturbance. Figure 5 shows the power spectral density of the performance variables $z(k)$ for the open-loop system and the closed-loop system after the controller parameters $\theta(k)$ converge. In the broadband frequency range between 10 and 20 Hz, peak attenuation exceeds 40 dB.

6. Experimental Results

In this section, retrospective cost adaptive disturbance rejection is demonstrated on the artificial white-light source of the DOT testbed. As described in Section 4, the tip and tilt of the fast-steering mirror are the controls $u(k)$. The optical position sensor provides two performance measures $z(k)$. Both performance measurements and the 2-axis measurements of the position of the fast steering-mirror are used as the feedback $y(k)$. The system disturbance is the ambient broadband noise in the laboratory. Up to 20 Hz, the ambient disturbance couples strongly into the dynamics of the artificial white-light source. Specifically, the ambient noise in the laboratory excites several of the modes of the white metrology tower, and thus disturbs the position of the artificial white-light source.

The retrospective cost adaptive controller is implemented on a dSpace DS1003/DS1004 combination board. Specifically, the algorithm is coded as a C++ S-function in Matlab and uploaded to the dSpace system. The algorithm is implemented with a sample rate of 1000 Hz with $n_c = 72$, $p = 2$, and $q = 3$. Four Markov parameters from the control input to the performance measure are required to construct H_{zu}. These four Markov parameters are identified using the observer/Kalman filter identification (OKID) algorithm described in [11, 12].

The power spectral densities of the performance signals are determined using an Agilent 35670A digital signal analyzer with a frequency window from 1 to 26 Hz, using 800 lines of resolution, and taking 25 averages. Figure 6 and Figure 7 provide power spectral densities of the two performance signals. The dotted lines are power spectral densities for the open-loop system, while the solid line provides power spectral densities for the closed-loop system after the adaptive controller $\theta(k)$ is allowed to converge. The adaptive controller achieves more than 15 dB of peak attenuation of a broadband disturbance in each performance measurement. Furthermore, the root-mean-square (rms) power spectral density of the z_1 performance signal is attenuated from -82.6 dB to -86.1 dB and the z_2 performance is attenuated from -82.4 dB to -86.7 dB closed-loop.

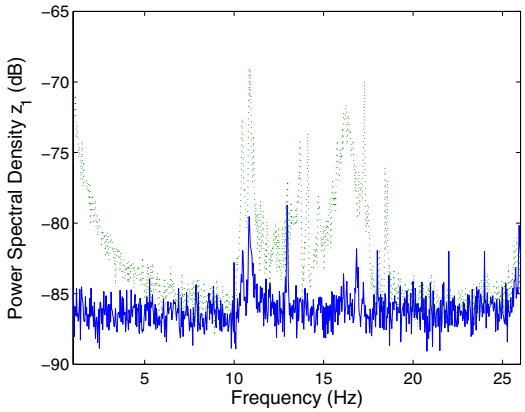

Fig. 6. Open-loop (dotted) and closed-loop (solid) power spectral density of z_1 experimentally determined using a digital signal analyzer. The adaptive controller achieves over 15 dB of peak attenuation of a broadband disturbance.

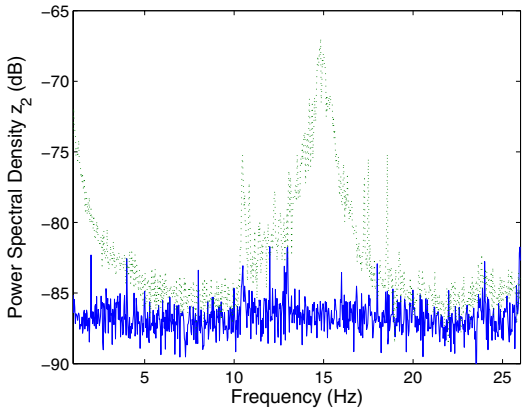

Fig. 7. Open-loop (dotted) and closed-loop (solid) power spectral density of z_2 experimentally determined using a digital signal analyzer. The adaptive controller achieves over 15 dB of peak attenuation of a broadband disturbance.

7. Conclusions

In this paper, we demonstrated broadband adaptive disturbance rejection on the artificial white-light source of the Deployable Optical Telescope developed by the Air Force Research Laboratory. We reviewed the discrete-time adaptive disturbance rejection algorithm presented in [9], and experimentally demonstrated its effectiveness in rejecting unknown broadband disturbances. The method is multi-input, multi-output and requires knowledge of some Markov parameters from the control input to the performance output. No information of the disturbance spectrum is required.

References

[1] K. D. Bell, R. L. Moser, M. K. Powers, and R. S. Erwin, "Deployable optical telescope ground demonstration," in *Proc. SPIE Vol. 4013: UV, Optical, and IR Space Telescopes and Instruments*, Munich, Germany, July 2000, pp. 559–567.

[2] K. N. Schrader, R. H. Fetner, J. Donaldson, R. J. Fuentes, and R. S. Erwin, "Integrated control system development for phasing and vibration suppression for a sparse-array telescope," in *Proc. SPIE Vol. 4849: Highly Innovative Space Telescope Concepts*, Waikoloa, HI, Dec 2002, pp. 134–145.

[3] K. N. Schrader, R. H. Fetner, S. F. Griffin, and R. S. Erwin, "Development of a sparse-aperture testbed for optomechanical control of space-deployable structures," in *Proc. SPIE Vol. 4849: Highly Innovative Space Telescope Concepts*, Waikoloa, HI, Dec 2002, pp. 384–395.

[4] S. M. Kuo and D. R. Morgan, *Active Noise Control Systems*. New York: Wiley, 1996.

[5] W. Messner and M. Bodson, "Design of adaptive feedforward algorithms using internal model equivalence," *Int. J. Adaptive Contr. Signal Processing*, vol. 9, pp. 199–212, 1995.

[6] P. A. Nelson and S. J. Elliot, *Active Control of Sound*. New York: Academic, 1992.

[7] L. A. Sievers and A. H. von Flotow, "Comparison and extensions of control methods for narrow band disturbance rejection," *IEEE Trans. Signal Processing*, vol. 40, pp. 2377–2391, 1992.

[8] R. Venugopal and D. S. Bernstein, "Adaptive disturbance rejection using ARMARKOV/Toeplitz models," *IEEE Trans. Contr. Sys. Tech.*, vol. 8, pp. 257–269, 2000.

[9] J. B. Hoagg and D. S. Bernstein, "Discrete-time adaptive feedback disturbance rejection using a retrospective cost measure," in *Proc. 2004 International Symposium on Active Control of Sound and Vibration*, Williamsburg, VA, Sept. 2004.

[10] T. McKelvey, H. Akcay, and L. Ljung, "Subspace-based multivariable system identification from frequency response data," *IEEE Trans. Autom. Contr.*, vol. 7, pp. 960–979, 1996.

[11] J. N. Juang, *Applied System Identification*. Upper Saddle River, NJ: Prentice-Hall, 1993.

[12] M. Phan, L. G. Horta, J.-N. Juang, and R. W. Longman, "Linear system identification via an asymptotically stable observer," *Journal of Optimization Theory and Application*, vol. 79, no. 1, pp. 59–86, 1993.